Integrated FBG Sensors Interrogation Using Active Phase Demodulation on a Silicon Photonic Platform

Yisbel E. Marin, Tiziano Nannipieri, Claudio J. Oton, and Fabrizio Di Pasquale

***Abstract*—The authors experimentally demonstrate the feasibility of interrogating Fiber Bragg Grating (FBG) sensors using an integrated unbalanced Mach–Zehnder Interferometer and active phase demodulation on silicon-on-insulator platform. The use of an external arrayed waveguide grating at the output of the circuit allows the interrogation of multiple FBGs through wavelength division multiplexing. Signal processing employing the phase-generated carrier demodulation technique is used to extract the wavelength shift from the signal patterns, allowing accurate dynamic FBG interrogation. The performance of the proposed integrated FBG interrogator is validated by comparing it with a commercial FBG readout unit based on a spectrometer and used as a reference. Experimental results demonstrate a dynamic strain resolution of 72.3 n$\varepsilon/\sqrt{\text{Hz}}$.**

***Index Terms*—Fiber Bragg Gratings (FBGs), Fiber sensors, high-volume manufacturing services, silicon on insulator, waveguides, wavelength meters, wavelength division multiplexing.**

I. Introduction

FIBER Bragg grating (FBG) sensors have shown great potential as a monitoring solution in a wide range of industrial fields, ranging from structural health monitoring to energy production, oil and gas, and transportation [1]. Their compactness, light weight, immunity to electromagnetic interference, and resistance to harsh environments gives them a clear advantage over conventional sensors. Additionally, the use of multiplexing techniques, such as time and wavelength-division multiplexing, allow monitoring multiple points along the same optical fiber. However, in order to make FBG sensors competitive with respect to conventional electronic sensors and satisfy high-volume market requirements, low-cost miniaturized readout units should be developed. The SOI platform allows the realization of high-density photonic integrated circuits (PIC) exploiting complementary metal–oxide–semiconductor compatible processes, including active and passive components [2], for a cost-effective dynamic interrogation of a very large number of FBGs.

FBG interrogation can be performed exploiting different configurations and techniques. Tunable lasers [3], spectral analysis [4], linear filters [5] and interferometers [6] are some examples. Many of these solutions require bulky and costly equipment. Recently, efforts towards the low-cost photonic integration of this kind of devices have been presented, such as the current-tuning of a VCSEL source [7], or the use of an arrayed waveguide grating as a spectrometer [8], [9]; however, these schemes also have some drawbacks, in particular regarding the number of FBGs that can be simultaneously interrogated and the dynamic capabilities of the readout unit.

In this paper, we present an integrated version of the scheme proposed in [6], which is based on an actively monitored unbalanced Mach–Zehnder interferometer (MZI) using phase-generated carrier (PGC) demodulation technique. This scheme allows to obtain two signals with 90° phase difference, from which the phase variations between the signals in each arm of the MZI can be extracted by applying techniques such as differentiation-and-cross multiplication and arctangent demodulation. The PGC demodulation helps overcome some of the MZI impairments, such as signal fading, identification of input signal direction, and fringe order ambiguity [10]. Although the proposed configuration along with the PGC technique have been used employing bulk components [11], it is the first time, to the best of our knowledge, that a dynamic strain measurement using an integrated FBG sensors interrogator has been demonstrated exploiting an actively monitored MZI on a silicon photonic platform.

The fabricated PIC includes input and output grating couplers that allow to vertically couple the signals reflected from the FBGs to the chip and the MZI output signals to external photodetectors. The feasibility of interrogating multiple FBGs simultaneously is demonstrated by employing an external arrayed-waveguide grating (AWG) device. The integration of photodetectors and AWGs on a SOI platform has been already demonstrated [2], [8], [9], and will be the subject of future developments.

II. Theory

Unbalanced MZI demodulators can be used to convert FBG sensors Bragg wavelength shift into phase variations of the output signal at the photodetector, allowing for very high resolution interrogation [10]. This type of MZIs is characterized by a differential length d between its arms. The spectral period of the fringe pattern is called the free spectral range (FSR) of the MZI. If the spectral width of the FBG is narrower than half the FSR of the MZI, an interference between these signals will be obtained at the output. This output signal can be written as:

$$I = A + B\cos\,\Delta\varphi(\mathrm{t}), \tag{1}$$

Manuscript received May 16, 2016; revised July 18, 2016 and August 1, 2016; accepted August 1, 2016. Date of publication August 4, 2016; date of current version June 24, 2017.

The authors are with the Scuola Superiore Sant'Anna, TeCIP Institute, Pisa 56124, Italy (e-mail: y.marin@sssup.it; t.nannipieri@sssup.it; c.oton@sssup.it; f.dipasquale@sssup.it).

Color versions of one or more of the figures in this paper are available online at http://ieeexplore.ieee.org.

Digital Object Identifier 10.1109/JLT.2016.2598395

where A is the DC component, B is proportional to the input intensity and depends on the mixing efficiency of the MZI, and $\Delta\varphi(t)$ is the phase difference between the signals in each arm of the MZI.

However, it is not straightforward to extract the precise phase condition only from the intensity of the output I, because the *arc cos* function has two solutions, and its responsivity varies along the fringe position. Active phase demodulation schemes like the PGC technique allow a precise estimation of the phase variations of the signal of interest by applying an external phase modulation on one of the MZI arms, with a frequency much higher than that of the signal of interest [11]. Considering a sinusoidal modulating signal with frequency ω_0 and amplitude C, the output (1) of the MZI becomes:

$$I = A + B\cos\left[C\cos\left(\omega_0 t\right) + \Delta\varphi(t)\right]. \tag{2}$$

This expression can be expanded in terms of Bessel functions, resulting in:

$$I = A + B\left\{\left[J_0\left(C\right) + 2\sum_{k=1}^{\infty}\left(-1\right)^k J_{2k}\left(C\right)\cos 2k\omega_0 t\right]\right.$$
$$\times\ \cos\Delta\varphi\left(t\right) - \left[2\sum_{k=0}^{\infty}\left(-1\right)^k J_{2k+1}\left(C\right)\cos\left(2k+1\right)\omega_0 t\right]$$
$$\left.\times\ \sin\Delta\varphi(t)\right\} \tag{3}$$

Equation (3) shows that by mixing the output of the MZI with the proper even and odd multiple of ω_0 and applying a low-pass filter to the signals to remove the frequencies above the band of interest, it is possible to obtain signals that are proportional to $\sin\Delta\varphi(t)$ and $\cos\Delta\varphi(t)$, from which the phase variations can be extracted by using, for example, the arc-tangent demodulation technique [12].

Considering mixing signals at ω_0 and $2\omega_0$, the ratio between the two signals at the output of the filters can be written as:

$$\frac{S_1}{S_2} = \frac{J_1\left(C\right)\sin\Delta\varphi\left(t\right)}{J_2\left(C\right)\cos\Delta\varphi\left(t\right)}, \tag{4}$$

where $J_1(C)$ and $J_2(C)$ are the Bessel functions of first and second order respectively, evaluated in C. From Bessel functions theory, the condition $J_1(C) = J_2(C)$ is satisfied when C is 0.84π [12], in which case the phase variations can be extracted by applying the arctangent method, as follows:

$$\Delta\varphi(t) = \arctan\left(\frac{S_1}{S_2}\right). \tag{5}$$

Finally, the phase change $\Delta\varphi(t)$ can be converted into wavelength shift $\Delta\lambda$ relative to the MZI FSR $\Delta\lambda_{FSR}$, using the relation:

$$\Delta\lambda = \frac{\Delta\lambda_{FSR}\Delta\varphi(t)}{2\pi}. \tag{6}$$

The same MZI can be used to monitor many different FBGs simply by wavelength demultiplexing its output. This means that only one modulator is needed to track the wavelength of many different gratings simultaneously.

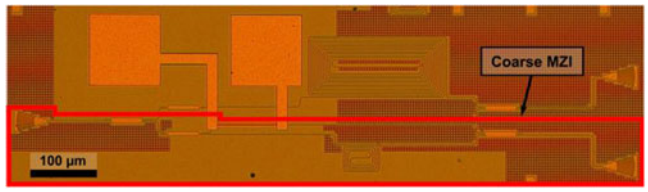

Fig. 1. Optical microscope image of the fabricated device. The total footprint is 1000 μm × 300 μm. Only the coarse MZI at the bottom, enclosed in red, was used in this work.

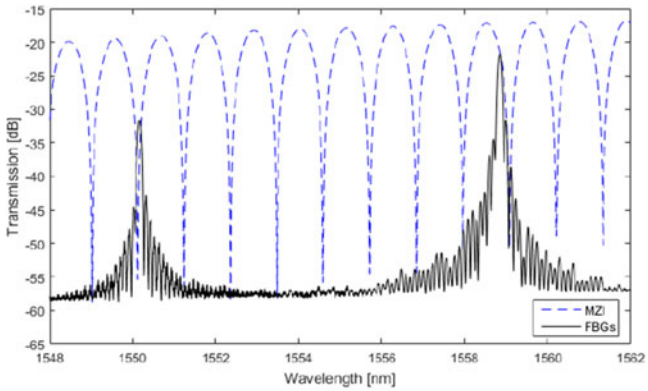

Fig. 2. Measured spectral response of the device and comparison with the FBG spectral width.

III. Design and Fabrication of the Device

The device (see Fig. 1) was fabricated from 8″ SOI wafers with 220 nm silicon thickness and 2 μm buried oxide. Deep-UV 193 nm optical lithography was used to pattern 220 nm × 480 nm single-mode waveguides. Focusing grating couplers were used for vertically coupling the light from single-mode fibers at 11°. A coupling loss of ∼5.5 dB per grating was measured from a reference sample. The photonic circuit includes two MZIs, one with path difference $\Delta L = 5000\,\mu$m (so-called fine), and another one with $\Delta L = 500\,\mu$m (so-called coarse), generating fringe patterns with FSRs of 0.11 and 1.1 nm respectively. The longer branches were spiraled to minimize footprint, resulting in a total circuit footprint of 1000 μm × 300 μm. Additionally, the short branch of both MZIs includes a thermal phase modulator, which consists in a metal Ti/TiN heater track which is 86 μm long and 1.4 μm wide. This modulator has a $1/e$ time-constant of 7 μs and a $V_{2\pi}$ of 3.6 V. Note that since the FBGs used are characterized by a full width at half maximum bandwidth of ∼80 pm, only the coarse MZI (with FSR 1.1 nm) could be used, as the FSR of the fine is too small (0.11 nm). Fig. 2 reports the measured spectral response of the MZI in comparison with the two FBGs spectral widths.

IV. Experimental Results

A. Experimental Setup

The experimental setup used for the dynamic characterization of the FBGs is shown in Fig. 3; the output of a wideband light source from BaySpec Inc. (centered at 1550 nm with a spectral width of 100 nm) was amplified using a high power EDFA and

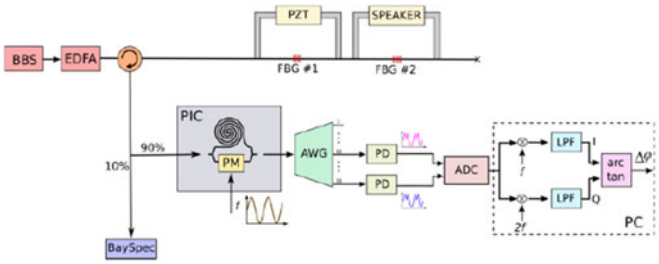

Fig. 3. Experimental Setup. BBS: Broadband Source; PZT: Piezo-Electric Actuator; PIC: Photonic Integrated Circuit; PM: Phase Modulator; AWG: Array Waveguide Grating; PD: Photodetector; ADC: Analog-to-Digital Converter; LPF: Low-Pass Filter; PC: Personal Computer.

then coupled to the FBGs under test using a three-port optical circulator. Two FBGs from FBGS Technologies GmbH were connected, one after the other. The first (FBG #1), characterized by a Bragg wavelength of ∼1558 nm, is longitudinally strained using an open loop piezo-electric actuator (PZT), whereas the second (FBG #2), with a Bragg wavelength of ∼1550 nm, is strained by the vibrations generated by a speaker. Both FBGs were actually pre-strained using a micrometer, in order to apply dynamic strain effectively, thus increasing the grating compression sensitivity. The reflection from the FBGs is divided using a 90/10 coupler; the 10% of the signal is sent to a commercial readout unit from Bayspec Inc., which has a maximum scanning frequency of 5 kHz/s, while the 90% part is coupled to the device under test. The output port of the chip is coupled to an external 16-channel AWG, characterized by a channel spacing of 200 GHz, which separates the signal into the different components reflected by each FBG. The channels employed were the 12th, centered at ∼1551 nm, which covers the band around FBG #2, and the 16th channel, centered at ∼1558 nm, which covers the band around FBG #1. Each channel is then coupled to an InGaAs based photoreceiver with a trans-impedance amplifier and 12 kHz bandwidth. Finally, the photoreceiver electrical signal is connected to a DAQ (100 kS/s) for data acquisition and processing on a PC.

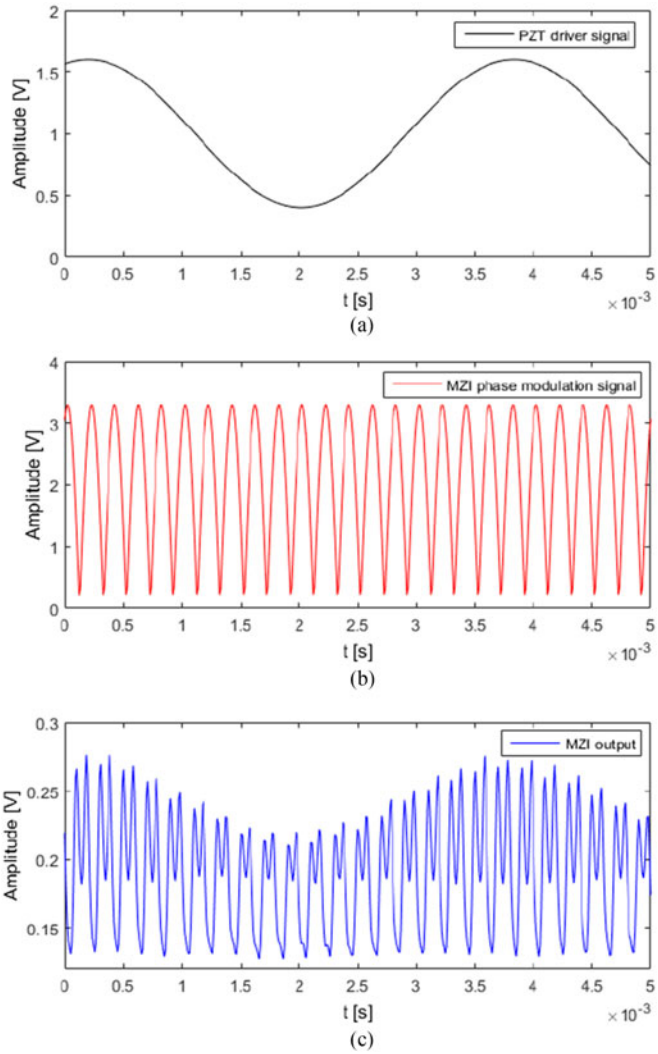

Fig. 4. Comparison between: (a) the signal driving the PZT controller, (b) the phase modulation signal applied to the MZI, and (c) the interferometer output detected by the photoreceiver.

B. Single FBG Interrogation

For the single FBG interrogation test, a sinusoidal signal of 275 Hz of frequency and 1.2 V peak-to-peak with 1 V DC component (see Fig. 4a) was applied to the PZT driver, which strains FBG #1, while no signal was applied to the speaker, to maintain FBG #2 static. Simultaneously, the resistor in one of the arms of the MZI was modulated using the square-root of a sinusoidal signal, since the applied power is proportional to the square of the voltage. The peak-to-peak amplitude was 3.3 V, which satisfies the condition $C = 0.84\,\pi$, and the frequency was 5 kHz (see Fig. 4b), which is more than ten times the frequency of variation of the Bragg wavelength.

The interferometer output detected by the photoreceiver (PD), corresponding to equation (2), is shown in Fig. 4(c). The slow varying envelope is due to the PZT driving signal (see Fig. 4a), while the fast amplitude variations are due to the MZI phase modulation signal (see Fig. 4b).

The comparison between the estimated wavelength shift, obtained after applying the technique explained in Section II, and the commercial FBG readout unit from BaySpec Inc. is reported in Fig. 5. Note that the device is capable of accurately measure variations of approximately 97 pm peak-to-peak, presenting a good agreement with the commercial readout unit results.

For the assessment of the minimum detectable wavelength no signal was applied to the PZT driver, for a static measurement, and the signal reflected by the FBG was detected using the MZI and BaySpec readout unit, as reported in Fig. 6. The standard deviation of the signal amplitude provides the minimum wavelength that can be detected by each device. For the MZI the value with a 1 kHz bandwidth is ∼1.98 pm whereas for the BaySpec is ∼0.33 pm. Considering a FBG strain sensitivity of 1.2 pm/$\mu\varepsilon$ at around 1.55 μm, these values are equivalent to a minimum detectable strain of ∼1.65 $\mu\varepsilon$ for the MZI and ∼0.28 $\mu\varepsilon$ for the BaySpec.

The spectra of the measured wavelength shift signals, normalized to the peak power of the BaySpec signal, are shown in Fig. 7. The harmonics observed in both spectra at 550 and 825 Hz are due to the hysteresis of the open loop PZT, which

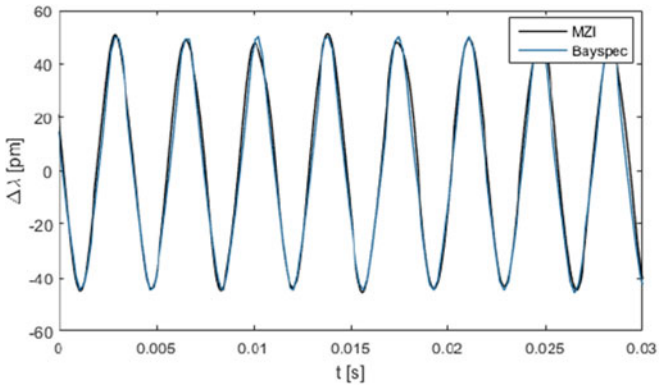

Fig. 5. Comparison of the measured wavelength shift versus time obtained with the device under test (in black) and the commercial FBG readout from BaySpec Inc. (in blue).

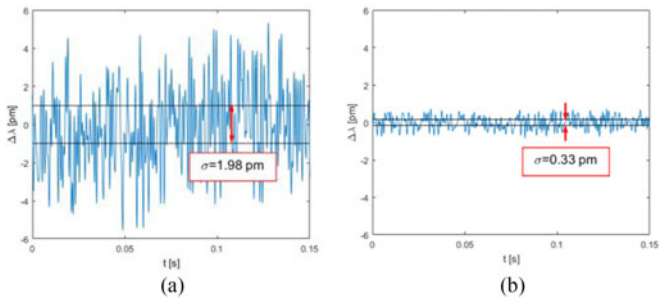

Fig. 6. (a) Fluctuations in the signal detected by the photodiode at the output of the MZI in absence of PZT driving signal. (b) Fluctuations detected by the BaySpec Inc. readout unit.

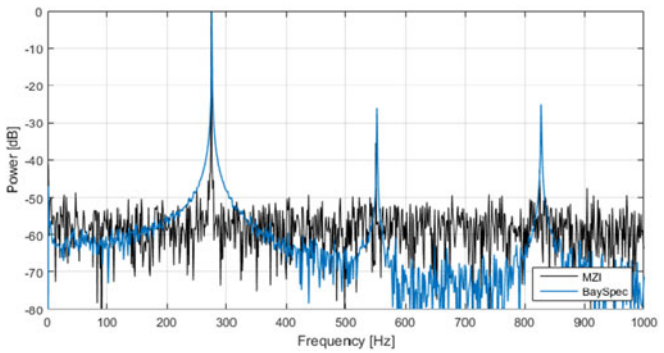

Fig. 7. Comparison of the spectra of the measured wavelength variation signals with the MZI and BaySpec Inc. readout unit.

causes the non-linearity of the displacement with respect to the applied sinusoidal voltage. The higher spectral width of the BaySpec signal with respect to the MZI signal could be due to lack of precision of the timestamp generated with the data of the readout unit, which could also justify the fact that the frequency peak is located slightly above 275 Hz. A signal-to-noise ratio (SNR) normalized to a 1-Hz bandwidth of approximately 51.9 dB was measured for the MZI, whereas for the BaySpec was approximately 69.9 dB, which results in a dynamic strain resolution of $72.3\,\mathrm{n}\varepsilon/\sqrt{\mathrm{Hz}}$ and $9\,\mathrm{n}\varepsilon/\sqrt{\mathrm{Hz}}$ respectively. The

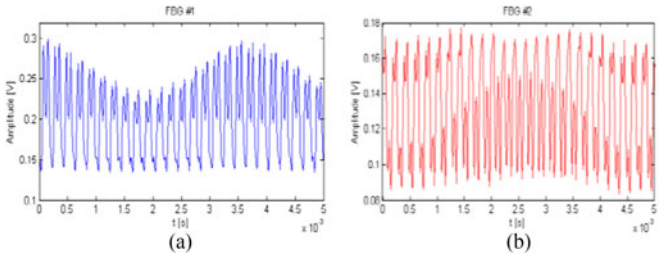

Fig. 8. AWG output signals detected by the photoreceivers.

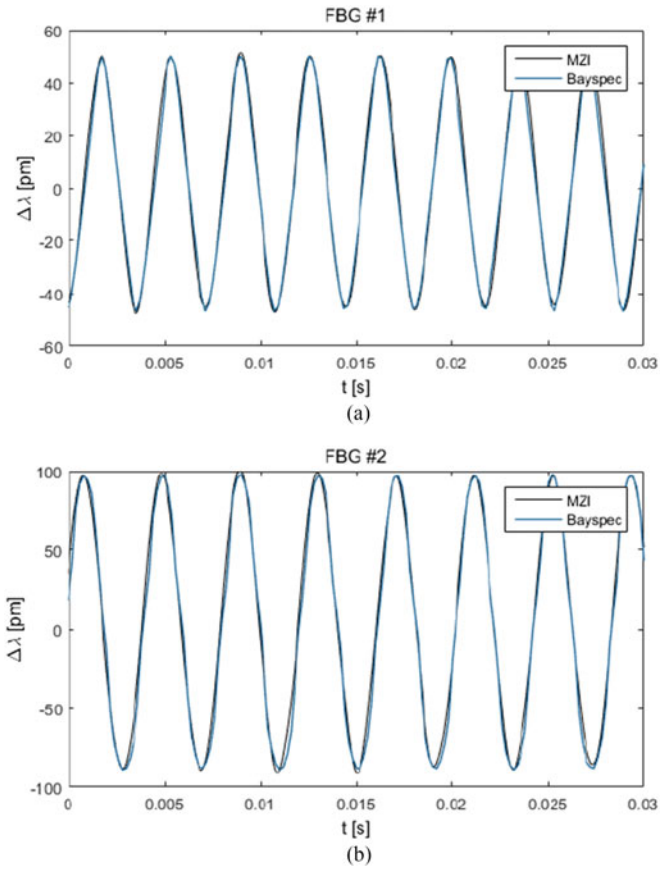

Fig. 9. Comparison of the measured wavelength shift versus time obtained with the device under test (in black) and the commercial FBG readout from BaySpec Inc. (in blue).

lower noise floor on the Bayspec spectrum with respect to the MZI is in agreement with the time-domain results depicted in Fig. 6(a) and (b), showing that the performance of the commercial readout unit by Bayspec is slightly better than the one of the proposed integrated solution, which could be due to the rather low signal intensity at the output of the external AWG with respect to the noise of the photoreceiver. The integration of the AWG and photoreceivers in the same chip would reduce the circuit losses by ∼10 dB, while the implementation of only the coarse circuit, without splitting the power between the coarse and fine configurations, would also provide a reduction in the total circuit loss, thus enhancing the SNR.

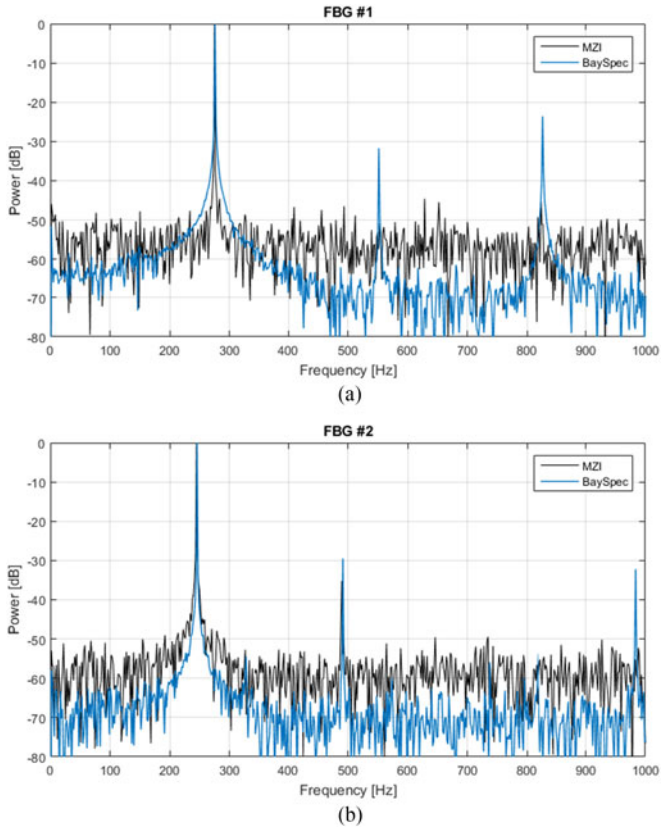

Fig. 10. Comparison of the measured wavelength shift versus time obtained with the device under test (in black) and the commercial FBG readout from BaySpec Inc. (in blue).

C. Multiple FBG Interrogation

For the multiple FBG interrogation test sinusoidal dynamic strains were applied simultaneously to the two FBG sensors; a sinusoidal signal at 275 Hz with 1.2 V peak-to-peak and 1 V DC component was applied to the PZT driver, which strains FBG #1, while a sinusoidal signal at 245 Hz with 0.5 V amplitude was applied to the speaker, which strains FBG #2. Simultaneously, one of the arms of the MZI was modulated using the square-root of a sinusoidal signal with an amplitude of 3.3 V, and a frequency of 5 kHz, which is more than ten times the frequency of variation of the Bragg wavelength of each FBG.

The signals detected at the output of the AWG are shown in Fig. 8. The signal in Fig. 8(a). was obtained from the 16th channel of the AWG, corresponding to the band of FBG #1, whereas the signal in Fig. 8(b) was obtained from the 12th channel of the AWG, corresponding to the band of FBG #2. Here it can be observed that the fast amplitude variations due to the MZI phase modulation coincide, while the slow variations are different, since each FBG is strained using signals with different frequencies and magnitudes.

The estimated wavelength shift for FBG #1 and FBG #2, and its comparison with the measurements obtained with the BaySpec are shown in Fig. 9(a) and (b) respectively. In both cases it was possible to meaure accurately the wavelength shift of ∼97 pm peak-to-peak for FBG #1, and ∼186 pm peak-to-peak for FBG #2.

The spectra of both signals are shown in Fig. 10. The SNR normalized to a 1-Hz bandwidth for FBG #1 is 50.83 dB while for FBG #2 is 54.53 dB, which results in a dynamic strain resolution of 82.1 $n\varepsilon/\sqrt{Hz}$ and 102.9 $n\varepsilon/\sqrt{Hz}$; for the BaySpec the SNR normalized to a 1-Hz bandwidth for FBG #1 strained at 275 Hz is 67.78 dB, corresponding to 11.71 $n\varepsilon/\sqrt{Hz}$, while the SNR for FBG #2 strained at 245 Hz is 78.73 dB, corresponding to 6.31 $n\varepsilon/\sqrt{Hz}$. The better SNR for the FBG #2 can be explained considering that the Bragg wavelength for FBG #2 corresponds to the band where the broadband source provides maximum power density, leading to a better SNR than in the tails of the source, where FBG #1 is located. Additionally, it can be observed from the spectra that there is no presence of crosstalk between the two AWG channels.

V. Conclusion

We presented an integrated FBG interrogator based on an actively monitored unbalanced MZI using the PGC technique. The device was fabricated on a SOI platform and it is capable of demodulating the wavelength shift variations of multiple FBGs simultaneously, by using an external AWG at the output of the MZI. The accuracy of the measurements was validated by comparing with a commercial readout unit, obtaining a very good agreement. The integration of the AWG and photoreceivers in the same SOI platform is envisaged to obtain a fully integrated readout unit, which could further improve the SNR of the demodulated signal.

References

[1] B. Culshaw and A. Kersey, "Fiber optic sensing: An historical perspective," *J. Lightw. Technol.*, vol. 26, no. 9, pp. 1064–1078, May 1, 2008.
[2] A. Ruocco and W. Bogaert, "Fully integrated SOI wavelength meter based on phase shift technique," in *Proc. IEEE 12th Int. Conf. Group IV Photon.*, Vancouver, BC, Canada, 2015, pp. 131–132.
[3] M. S. Müller *et al.*, "Fiber-optic sensor interrogation based on a widely tunable monolithic laser diode," *IEEE Trans. Instrum. Meas.*, vol. 59, no. 3, pp. 696–703, Mar. 2010.
[4] P. Niewczas, A. J. Willshire, L. Dziuda, and J. R. McDonald, "Performance analysis of the fiber bragg grating interrogation system based on an arrayed waveguide grating," *IEEE Trans. Instrum. Meas.*, vol. 53, no. 4, pp. 1192–1196, Aug. 2004.
[5] R. Beccherelli *et al.* "Fiber Bragg grating interrogation system based on a novel integrated optical filter," in *Proc. IEEE Sensors*, 2008, pp. 140–143.
[6] A. D. Kersey, T. A. Berkoff, and W. W. Morey, "High-resolution fibre-grating based strain sensor with interferometric wavelength-shift detection," *Electron. Lett.*, vol. 28, no. 3, pp. 236–238, 1992.
[7] B. Van Hoe *et al.*, "Ultra small integrated optical fiber sensing system," *Sensors*, vol. 12, no. 9, pp. 12052–12069, 2012.
[8] A. Trita *et al.*, "Simultaneous interrogation of multiple fiber bragg grating sensors using an array waveguide grating filter fabricated in SOI platform," *IEEE Photon. J.*, vol. 7, pp. 1–11, no. 6, Dec. 2015.
[9] H. Li, W. Gao, E. Li, and C. Tang, "Investigation of ultrasmall 1 x N AWG for SOI-Based AWG demodulation integration microsystem," *IEEE Photon. J.*, vol. 7, no. 6, 2015.
[10] S. Yin, P. B. Ruffin, and F. T. S. Yu, "Interrogation techniques for FGSs and the theory of fiber gratings," in *Fiber Optic Sensors*, 2nd ed., Boca Raton, FL, USA: CRC Press, 2008.
[11] A. Dandridge, A. B. Tveten, and T. G. Giallorenzi, "Homodyne demodulation scheme for fiber optic sensors using phase generated carrier," *IEEE Trans. Microw. Theory Techn.*, vol. 30, no. 10, pp. 1635–1641, Oct. 1982.

Yisbel E. Marin received the B.Sc. degree in electronic engineering from the Universidad Nacional Experimental Politecnica "Antonio Jose de Sucre," Barquisimeto, Venezuela, in 2010, and the M.Sc. degree in photonic networks engineering from both Aston University, Birmingham, U.K., and Scuola Superiore Sant'Anna, Pisa, Italy, in 2015. She is currently working toward the Ph.D. degree in emerging digital technologies, photonic technologies curriculum in the Institute of Information Communication and Perception Technologies, Scuola Superiore Sant'Anna. Her current research interests are optical fiber sensors and photonic integrated circuits.

Tiziano Nannipieri was born in Pisa, Italy, in 1980. He received the Laurea degree (B.S.) and the Laurea Magistralis degree (M.S.) in telecommunications engineering from the University of Pisa, Pisa, Italy, in 2007 and 2008, respectively. From 2009 to 2010, he was Consorzio Nazionale Interuniversitario per le Telecomunicazioni (CNIT) scholarship student at the National Laboratory of Photonic Networks, Pisa. He is currently in the Optical Fiber Sensors and Integrated Photonics Subsystems Research Area, Institute of Communication, Information and Perception Technologies, Scuola Superiore Sant'Anna, Pisa. His research interests are in the area of fiber optic sensing, especially in design and development of distributed and discrete fiber optic sensor systems for multiparameter physical sensing based on Raman, Brillouin and Rayleigh scattering as well as Fiber Bragg Gratings.

He is an author and a co-author of more than 20 scientific journals and conference papers in the area of optical fiber sensors and is a reviewer of IEEE/OSA SENSORS JOURNAL, *Optics Express*, *Optics Letters*, and *Applied Optics*.

He is a co-founder and an R&D Engineer of INFIBRA TECHNOLOGIES, a Scuola Superiore Sant'Anna spin-off company engaged in different sectors ranging from Oil&Gas to Transportation with its own advanced fiber optic sensor systems.

Claudio J. Oton received the Ph.D. degree in 2005 from the University of La Laguna, San Cristóbal de La Laguna, Spain. Then, he spent four years in the Optoelectronics Research Centre, Southampton, U.K., where he worked on integrated optical amplifiers and lasers on silicon as a Marie Curie postdoctoral fellow. In 2009, he joined Nanophotonics Research Centre, Universidad Politecnica de Valencia, Valencia, Spain, where he studied nonlinear silicon photonic devices. Finally, from 2012 he is an Assistant Professor in TeCIP Institute, Scuola Superiore Sant'Anna, Pisa, Italy. He is an author of more than 60 peer-reviewed scientific papers and several conference contributions, which yield an *h*-index of 22. His current research interests include optical fiber sensors and silicon photonic integrated devices.

Fabrizio Di Pasquale received the degree in electronic engineering from the University of Bologna, Bologna, Italy, in 1989 and the Ph.D. degree in information technology from the University of Parma, Parma, Italy, in 1993. From 1993 to 1998, he was in the Department of Electrical and Electronic Engineering, University College London, London, U.K., as a Research Fellow, working on optical amplifiers, wavelength division multiplexing (WDM) optical communication systems and liquid crystal displays. After two years with Pirelli Cavi e Sistemi and two years with Cisco Photonics Italy, he moved to Scuola Superiore Sant'Anna, Pisa, Italy, where he is currently a Full Professor of telecommunications. His current research interests include optical fiber sensors, silicon photonics, optical amplifiers, WDM transmission systems, and networks. He is a Co-Founder and the President of INFIBRA TECHNOLOGIES, a spin-off company of Scuola Superiore Sant'Anna, developing and marketing advanced fiber optic sensor systems.

He has filed 20 international patents and he is the author and a co-author of more than 200 scientific journals and conference papers. He is on the Board of Reviewers of IEEE PHOTONICS TECHNOLOGY LETTERS, IEEE/OSA JOURNAL OF LIGHTWAVE TECHNOLOGY, IEEE SENSORS JOURNAL, *Optics Communications*, *Optics Express*, and *Optics Letters*.